Received Date : 04-Dec-2015
Accepted Date : 15-Jan-2016
Article type : Primary Research Articles

The value of crossdating to retain high-frequency variability, climate signals, and extreme events in environmental proxies

Running title: Dating control in environmental proxies

Bryan A. Black[1*], Daniel Griffin[2], Peter van der Sleen[1], Alan D. Wanamaker Jr.[3], James H. Speer[4], David C. Frank[5], David W. Stahle[6], Neil Pederson[7], Carolyn A. Copenheaver[8], Valerie Trouet[9], Shelly Griffin[3], and Bronwyn M. Gillanders[10]

[1] Marine Science Institute, University of Texas at Austin, 750 Channel View Drive, Port Aransas, TX 78373, USA.
[2] Department of Geography, Environment, and Society, University of Minnesota, Geography Room 414, Minneapolis, MN 55455, USA.
[3] Department of Geological and Atmospheric Sciences, Iowa State University, 12 Science I, Ames, IA 50011, USA.
[4] Department of Earth and Environmental Systems, Indiana State University, Science 159E, Terre Haute, IN 47809, USA.
[5] Swiss Federal Research Institute WSL, Zürcherstrasse 111, CH-8903 Birmensdorf, Switzerland and Oeschger Centre for Climate Change Research, University of Bern, Zähringerstrasse 25, CH-3012 Bern, Switzerland.
[6] Department of Geosciences, University of Arkansas, 216 Ozark Hall, Fayetteville, AR, 72701, USA.
[7] Harvard Forest, 324 N Main St., Petersham, MA 10366, USA.
[8] Department of Forest Resources and Environmental Conservation, Virginia Tech, 228C Cheatham Hall, Blacksburg, VA, 24061, USA.

[9] Laboratory of Tree-Ring Research, University of Arizona, 1215 E. Lowell St., Tucson, AZ, 85721, USA.

[10] School of Biological Sciences & Environment Institute, University of Adelaide, Darling Building, Adelaide, South Australia, 5005, Australia.

*Corresponding author: Bryan Black; bryan.black@utexas.edu; 361-749-6789

Keywords: crossdating, dendrochronology, sclerochronology, climate reconstruction, paleoclimate, global change

Primary Research Article

Abstract

High-resolution biogenic and geologic proxies in which one increment or layer is formed per year are crucial to describing natural ranges of environmental variability in Earth's physical and biological systems. However, dating controls are necessary to ensure temporal precision and accuracy; simple counts cannot ensure that all layers are placed correctly in time. Originally developed for tree-ring data, crossdating is the only such procedure that ensures all increments have been assigned the correct calendar year of formation. Here, we use growth-increment data from two tree species, two marine bivalve species, and a marine fish species to illustrate sensitivity of environmental signals to modest dating error rates. When falsely added or missed increments are induced at one and five percent rates, errors propagate back through time and eliminate high-frequency variability, climate signals, and evidence of extreme events while incorrectly dating and distorting major disturbances or other low-frequency processes. Our consecutive Monte Carlo experiments show that inaccuracies begin to accumulate in as little as two decades and can remove all but decadal-scale processes after as little as two centuries. Real-world scenarios may have even greater consequence in the absence of crossdating. Given this sensitivity to signal loss, the fundamental tenets of crossdating must be applied to fully resolve environmental signals, a point we underscore as the frontiers of growth-increment analysis continue to expand into tropical, freshwater, and marine environments.

Introduction

Instrumental and observational environmental records are generally limited to the past 150 years and thus do not fully capture natural ranges of variability in Earth's physical and biological systems (IPCC AR5). However, these histories can be extended by orders of magnitude using such proxies as speleothems, ice cores, sediments, boreholes, and growth

increments (tree rings, fish otoliths, corals, and bivalves) to benchmark pre-industrial conditions, quantify low-frequency processes, and provide context for interpreting modern trends. Multi-decadal to multi-centennial histories also increase the probability of capturing rare, extreme events and severe disturbances that can profoundly alter ecosystem productivity and functioning (Foster *et al.*, 1998; Ciais *et al.*, 2005; Jackson *et al.*, 2009; Reichstein *et al.*, 2013).

Although proxies can provide longer histories than instrumental records, they require dating controls to ensure that the resulting environmental reconstructions are accurately placed in time. Various radiometric techniques (such as ^{210}Pb, ^{14}C, U-Th and many others) can be employed, as can time-specific signatures such as volcanic horizons, turbidites, or fallout from nuclear weapons testing (Baumgartner *et al.*, 1989; Austin *et al.*, 1995; Weinheimer & Biondi, 2003; Vinther *et al.*, 2006; Scourse *et al.*, 2012). Layer counts may also be used as a dating tool if the proxy consists of periodic bands, as would be the case for annually varved sediments or growth increments in biological archives, and some laminae in spleothems (Baker *et al.*, 1993). Under favorable circumstances, this may better constrain dating than some radiometric techniques, especially radiocarbon, for which associated chronological errors can be more than ± 50 years (Scott *et al.*, 2007; Lowe & Walker, 2015). However, there is still an undetermined error rate caused by incorrectly identified or missed bands with cumulative effects that propagate back through time. Lower-frequency signals may be preserved, but higher-frequency, interannual signals likely will become muted or offset in time, especially in the early portion of the reconstruction (Baumgartner *et al.*, 1989; Fritts & Swetnam, 1989).

Originally developed for tree-ring data, crossdating provides a means by which to control error and generate reconstructions that are fully annually-resolved (one value per year) and exactly placed in time (Glock, 1937; Douglass, 1941; Fritts, 1976; Stokes & Smiley, 1996). This procedure is based on the assumption that some aspect of the environment limits tree growth, and as it varies, induces a synchronous pattern or growth 'bar code' among samples of a given species and location (Fritts, 1976; Speer, 2010). Beginning with living samples, the synchronous growth pattern is cross-matched backward through time starting at the increment formed during the known year of collection. If an increment has been missed or falsely identified, the growth pattern in that individual will be offset by a year relative to the other individuals in the sample, beginning where the error occurred. The location of the dating error is then confirmed by re-examining the wood for the presence of a false, missing, or partial increment.

Ultimately, crossdating is a process of hypothesis testing among individual samples to correctly identify irregularities, and with results that can be quantified and replicated among practitioners. High-frequency (interannual) signals are captured in the final chronology, facilitating the integration of tree-ring data with instrumental or historical records and maximizing accuracy in environmental reconstructions. Moreover, samples with unknown death dates from historical structures, bogs, or the forest floor may be crossdated among one another or with live-collected samples to yield chronologies that far exceed the lifespan of individual trees. Considering that forests are broadly distributed and easily accessible, annually resolved tree-ring chronologies are leading indicators of long-term forest dynamics, climate, and impacts of human land use across a range of temporal and spatial scales. The global network held in the International Tree-Ring Databank now includes more than 4,300 chronologies, enabling syntheses across stands, landscapes, and hemispheres (Grissino-Mayer & Fritts, 1997; St George, 2014).

Beyond trees, an expanding frontier in crossdating is its application to increments of long-lived animal species including fish, bivalves, and corals (Cobb *et al.*, 2003; Black *et al.*, 2005; Butler *et al.*, 2013; DeLong *et al.*, 2014; Mette *et al*., 2016). Resulting chronologies can be used among other applications to i) estimate the impacts of climate variability on growth, ii) disentangle human and environmental impacts, iii) generate ecosystem indicators, iv) establish linkages within and across ecosystems and ocean domains, v) reconstruct climate prior to the beginning of the instrumental record, and vi) estimate population age structure. Chronologies and associated age data can be of particularly high value in aquatic ecosystems, especially in the oceans, where the cost of repeated sampling is prohibitively high and multidecedal time series are consequently rare. Crossdating of annual layers remain less common in speleothems, annual varves, corals, and ice cores, though this is often due to the difficulty of collecting multiple replicates (Comboul *et al.*, 2014).

Despite its widespread implementation in tree-ring records and the recent rise of new datasets and disciplines, the importance of crossdating to signal retention remains poorly quantified. To this end, we assemble crossdated growth-increment data from several marine and terrestrial species that represent a diversity of habitats and life histories and then induce dating errors at conservative rates. In so doing, we illustrate the importance of crossdating by documenting the extent to which synchronous environmental signals are degraded, especially

high-frequency variability, climate-growth relationships, and the frequency and magnitude of extreme events.

Materials and Methods

Datasets

Five datasets are included in the analysis, three of which have been previously published. Two are terrestrial: a blue oak (*Quercus douglasii*) stand from southern California (Stahle *et al.*, 2013) and a Douglas-fir (*Pseudotsuga menzeisii*) stand from the western Cascade Mountains of Oregon (Table 1). The remaining datasets are marine, including the bivalve species *Arctica islandica* from the central coast of Maine, USA, the bivalve species Pacific geoduck (*Panopea generosa*) from the northern British Columbia coast, Canada, (Black *et al.*, 2009), and splitnose rockfish (*Sebastes diploproa*) from the north-central California Current, USA (Black *et al.*, 2011; Black *et al.*, 2014). Increments (used interchangeably here for "rings") were examined in cores and cross sections for trees, acetate peels for Pacific geoduck (Black *et al.*, 2008b) and *Arctica* shells (Griffin, 2012), and otolith thin sections for splitnose rockfish (Black *et al.*, 2005). All otolith and bivalve samples had been photographed at approximately 50 – 100 times magnification under a dissecting microscope (Black *et al.*, 2011; Griffin, 2012).

All datasets were visually crossdated using skeleton plotting and list-year techniques (Stokes & Smiley, 1996; Speer, 2010), after which otolith and bivalve increment widths were measured using Image Pro Plus v. 9.1 while tree-ring widths were measured to the nearest 0.001 mm using a Velmex TA Tree-Ring measuring system. In the *Arctica* and blue oak datasets, dead individuals from the ocean or forest floor had been collected to extend the chronology as far back in time as possible. However, we felt it was unrealistic that dead-collected material could be accurately crossdated into a chronology that contains dating errors, as is simulated here. The same was true for several geoduck that had distorted edges in which the most recent decades could not be crossdated. Thus, only live-collected samples with increments that could be measured to the most recent years of growth were retained. The extent to which dating errors compromise the ability to crossdate dead-collected material is more fully addressed later in the study.

Upon completion of visual crossdating and growth-increment measurement, crossdating was statistically verified using the computer program COFECHA in which the high-frequency growth pattern of each measurement time series was isolated and cross-correlated with the

average growth pattern of all others in the sample set (Holmes, 1983; Grissino-Mayer, 2001). Any low ($p > 0.01$) correlations pointed to a possible dating error and any such samples were re-inspected. The mean correlation between each measurement time series and the average of all others was reported as the series intercorrelation, which is a common metric of dating accuracy and growth synchrony (Grissino-Mayer, 2001; Speer, 2010).

All five species exhibited age-related growth declines, which were removed by fitting each individual with a negative exponential, negative linear function, or horizontal line and then dividing observed by predicted values. Detrending standardized each set of measurements to a mean of one and helped stabilize variance, which also tended to decline with age. All detrending was conducted in the computer program ARSTAN (Cook & Holmes, 1986; Cook & Krusic, 2005; LDEO, 2015). The Expressed Population Signal (EPS) was used to quantify how well the chronology developed from a given number of samples (trees, fish, or bivalves) represents the theoretical population (Wigley *et al.*, 1984). Its calculation involves the number of samples contributing to a chronology (n) and the mean correlation among these samples ($\bar{r}$) where $EPS = (n \times \bar{r}) / ((1 + (n-1)) \bar{r})$. A higher $\bar{r}$ (i.e. stronger synchrony among samples) and greater sample depth can each increase EPS. Albeit arbitrary, an $EPS \geq 0.85$ is often used as a threshold at which the chronology is considered sufficiently robust for climate reconstruction. The EPS was especially useful at demonstrating the loss of common signal from a chronology as error rates increased.

Error simulation

Detrended measurement time series were pooled and an average of one error per 100 rings (1% rate) was applied after which a second analysis was conducted where an average of five errors per 100 rings (5% rate) was applied. Eighty percent of these errors were designated as missing rings and 20% were designated as false rings. Thus, to simulate a 1% error rate, 100 errors would be introduced into a dataset with 10,000 ring-width index values, 80 of which would be missing rings and 20 of which would be false rings. Missing rings were simulated by combining the selected increment with the one immediately prior, and then shifting forward by one calendar year all preceding increments in the measurement time series. In the absence of crossdating, unusually narrow and locally absent rings tend to be missed with the greatest frequency. To simulate this effect, the lowest percentile of ring-width index values were

assigned approximately four times the chance of being missed, decreasing to approximately twice the chance of being missed for those ring-width index values in the fifth percentile. All other ring width index values had a random chance of being missed.

False rings were simulated by dividing the selected increment in half to form two increments, and then shifting backward by one calendar year all preceding increments in the measurement time series. Growth increment boundaries are generally the most challenging to interpret in early biological age, and this is therefore where false rings (or "checks" as false rings are termed in sclerochronology) most commonly occur (Schulman, 1939; Black *et al.*, 2008b; Butler *et al.*, 2009; Copenheaver *et al.*, 2010a; Edmondson, 2010). To simulate this effect, the first ring-width index values of the measurement time series were assigned approximately four times the chance of being identified as false, decreasing exponentially through the first hundred years. All ring-width index values more than 100 years into the time series had a random chance of being identified as false. Many individuals, especially fish and bivalves, were less than 100 years old, but this approach still provided a means by which to weight initial growth with a relatively higher amount of false rings. Overall, it should be noted that true missing (locally absent) or false rings were not necessarily present in these datasets. The goal was to simulate the tendency to skip rings that may actually be present or add rings that were not present, as can often occur in the absence of crossdating and careful interpretation of the wood or carbonate structures. Past experience suggests that unusually narrow increments tend to be skipped while false additions tend to occur in wide rings.

In total, one hundred iterations of the error simulation program were performed for each dataset. The 100 ensemble "error" chronologies were averaged into a composite chronology that highlighted the mean effect of dating errors. Probability density functions were calculated for the values of each crossdated and composite error chronology using kernel density estimation. All error simulations and probability density function analysis were conducted in the program SAS v. 9.4, SAS Institute, Inc. Cary, NC. Cross-wavelet coherence analysis (Grinsted *et al.*, 2004) was used to compare the correctly crossdated chronology with the composite chronologies at 1% and 5% error rates. Roughly analogous to correlation, the cross wavelet plot illustrates coherence and phase between two time series as a function of both time and frequency. Wavelet analysis was performed using MatLab, MathWorks, Natick, MA.

Climate-growth relationships and detection of extreme events

The crossdated chronologies and the error composite chronologies were next related to instrumental climate records. Three species were chosen based on previous studies that had demonstrated strong climate-growth relationships. Pacific geoduck (Strom *et al.*, 2004; Black *et al.*, 2009) was correlated with the leading principal component of mean annual sea surface temperatures from lighthouse stations along the British Columbia coast (Black *et al.*, 2009) as well as Hadley ISST 1° gridded mean annual sea surface temperature. Splitnose rockfish (Black *et al.*, 2011; Black *et al.*, 2014) was correlated with mean January through March upwelling index averaged across 36°N and 39°N as well as mean January through March 1° gridded Hadley ISST sea surface temperature. Blue oak (Stahle *et al.*, 2013) was correlated with prior December through current February NOAA NCDC CA Divisions 5 and 7 precipitation as well as 1° gridded Hadley prior December through current February precipitation. Correlation analysis with gridded Hadley data was performed in the KNMI Climate Explorer (Trouet & Van Oldenborgh, 2013).

The extent to which dating error degraded the ability to detect extreme events was evaluated using the blue oak dataset. First, the crossdated chronology and each of the 100 error chronologies at the 1% and then 5% error rates were normalized to a mean of zero and a standard deviation of one. An extreme event was defined as any period in which the normalized crossdated chronology exceeded a value of plus or minus two. The percentage of error chronologies that also exceeded two (correct detection) was calculated as was the percentage of error chronologies that exceeded two during other calendar years (false positives).

Addition of "floating" material

Samples with an unknown date of death ("floating" measurement time series) can be crossdated into a chronology generated from live-collected individuals, assuming there is sufficient overlap in time. In trees and bivalves, this approach has been used to develop chronologies that greatly exceed the lifespan of an individual (Pilcher *et al.*, 1984; Ferguson *et al.*, 1985; Becker, 1993; Friedrich *et al.*, 2004; Scourse *et al*., 2006; Butler *et al*., 2013). Here, we examine the extent to which dating errors reduce the ability to correctly place floating samples in time using the blue oak, geoduck, and Douglas-fir datasets. Three samples were selected for each species, spanning 1691-1885, 1787-1890, and 1732-1867 for blue oak, 1917-

1969, 1918-1959, and 1922-1971 for geoduck, and 1350-1450 for all three Douglas-fir. The three blue oak samples were dead collected while the three geoduck samples were live collected, but from individuals with edges so distorted that the most recent decades could not be crossdated or measured. None of these blue oak or geoduck samples had been included in the master chronologies used for error simulation. There were no dead-collected individuals for Douglas-fir, so three measurement time series included in the original simulation analysis were used. However, the simulation analysis was re-run three times, each excluding one of the three measurement time series to avoid comparing a measurement time series with itself.

The crossdated chronology, each of the 100 chronologies generated with a 1% error rate, each of the 100 chronologies generated with a 5% error rate, and the three floating measurement time series were detrended using splines with 50% frequency cutoff at 20 years, which isolated high-frequency variability. A correlation coefficient was calculated between each of three detrended floating samples and i) the crossdated chronology, ii) each of the 100 chronologies generated with a 1% error rate, and iii) each of the 100 chronologies generated with a 5% error rate. Correlations were also calculated from plus or minus one to plus and minus twenty year lags from the floating sample's correct (lag 0) position in time. A clear, unambiguous peak correlation occurring at lag 0 would provide compelling evidence that a floating time series had been correctly placed in time. Note that errors were not induced into the floating time series to provide a conservative, best-case scenario.

Results

Data properties varied widely among species; time series length for Douglas-fir was an order of magnitude longer than that of splitnose rockfish (Table 1). Also, the degree of synchrony among measurement time series, as indexed by the series intercorrelation, varied widely from a minimum of 0.58 to a maximum of 0.84 (Table 1). The introduction of error profoundly masked synchrony, as illustrated by a single iteration of the 5% error simulation in which close alignment of the crossdated measurement time series was almost completely lost (Fig. 1a,b). The full ensemble of 100 error chronologies and their mean (the composite chronology) further illustrated the loss of accuracy, especially in high-frequency domains (Fig. 1c). Indeed, this composite chronology became increasingly smoothed and forward-offset (shifted toward the right) as the innermost date of 1787 was approached (Fig. 1c).

277 The smoothing effects of dating inaccuracy were greatest at the 5% rate, and in the
278 earliest portions of the longest datasets, notably Douglas-fir (Fig. 2b). Impacts of dating errors
279 were also still apparent at the 1% rate, and even in the shorter-lived bivalve and fish species (Fig.
280 2). This was most evident in years with extreme values, for example 1998 in splitnose rockfish
281 or 1941 in geoduck. In these cases, variance in the error composite chronologies was muted
282 relative to the crossdated chronology, and these impacts were most pronounced early in the
283 dataset (Fig. 2). Probability density functions provided another means by which to illustrate how
284 extreme values were lost and distributions became increasingly centered on a value of one as
285 error increased (Fig. 2). As another consequence of error, the percentage of correctly dated
286 measurement time series diminished back through time, dropping below 50% in just a few
287 decades (Fig. 2).
288 Cross-wavelet analysis more fully quantified the timing of differences between the
289 crossdated and composite chronologies, as well as the specific wavelengths involved. For blue
290 oak, Douglas-fir, and the two bivalve chronologies, the crossdated and 5% error composite
291 chronologies were largely coherent over recent decades (Fig. 3). By the mid-20th century,
292 differences between the two became evident in the higher-frequency domains (<4 yr), eventually
293 extending into lower-frequency domains (8-16 yr) farther back in time. This was especially true
294 for Douglas-fir, which accumulated errors over its 700-year span that affected even the very low-
295 frequency variability (>100 yr) (Fig. 3b). Note that in the early portions of the Douglas-fir
296 dataset (1200s-1400s), the wavelet analysis identified signals common to both the crossdated and
297 error composite chronologies. However, most of these were out of phase with one another, as
298 illustrated by left-facing arrows. The error chronology had become offset to the extent that low-
299 frequency signals were the inverse of those in the crossdated chronology (Fig. 3b). In contrast to
300 the other datasets, the crossdated and error composite chronology for splitnose rockfish differed
301 across a range of wavelengths in the most recent decades, especially 1975-2005 (Fig. 3e). For all
302 species, differences between the crossdated and error composite chronology were less
303 pronounced at the 1% error rate (Fig. S1).
304 Error reduced EPS relative to each crossdated chronology, and the decrease in EPS
305 became more pronounced farther back through time (Fig. S2). Effects were most evident at the
306 5% error level, but even the 1% error rate caused EPS to prematurely drop below a value of 0.85
307 (Fig. S2). This loss of synchronous, high-frequency signal resulted in significantly lower

correlations with climate variables (Fig. 4). In blue oak, geoduck, and splitnose rockfish, the correlations between climate and 1% or 5% error chronologies were significantly ($p < 0.05$) lower than the correlations between climate and the crossdated chronology (Fig. 4a-c). The reduction in correlation was somewhat subtle at the 1% level, but was much more severe at the 5% rate (Fig. 4a-c). This loss of signal at the 5% error rate was also apparent in gridded climate datasets for which the intensity and extent of correlations was markedly reduced in comparison to the crossdated chronology (Fig. 4d-i). Moreover, the ability to identify extreme events was severely compromised (Fig. 5). Although data with a 1% error rate successfully captured extreme events after approximately 1850, there was a high number of false positives that would have induced considerable inaccuracy in any reconstruction (Fig. 5b). There was no ability to correctly identify extremes at the 5% error rate (Fig. 5c).

Errors also reduced the ability to exactly place "floating" samples in time. For each of the three species examined, correlations between the crossdated chronology and each of the three floating samples rose to a sharp, well-defined peak at their correct placement in time at lag zero (Fig. S3). With the exception of geoduck, correlations between the floating time series and the 1% error chronologies were reduced in comparison to correlations with the crossdated chronology (Fig. S3 a,c,e). These effects were strongly evident at the 5% error rate for which correlations were considerably lower and no clear peak occurred at any lag (Fig. S3 b,d,f).

Discussion

Estimates of error rates in the absence of crossdating

Dating errors profoundly muted and also blurred in time the synchronous environmental patterns contained within the original growth-increment data. Overall, the error rates used to generate these results were probably conservative, though error frequency is rarely reported in the literature. Studies that do not employ crossdating have no basis with which to gauge error rates while those that do employ crossdating visually eliminate errors before they can be quantified. However, some general estimates are available. In an earlier study, 27 *Arctica* from the Maine site were found to have an average error rate of 4% (ranging from 0 to 27%) when measured without crossdating (Griffin, 2012). In another example, error rates in geoduck ring counts almost always exceed 5% and could be as high as 30% in older (>100 yr) individuals (Black *et al.*, 2008b), comparable to or higher than the rates used in the present analysis. In

general, these error rates cited for *Arctica* and geoduck are almost certainly best-case scenarios given that they involved well prepared samples and experienced researchers.

Equivalent data were not readily available for trees, though frequencies of false rings or locally absent rings may provide some minimum error estimates. Locally absent rings occur when an increment does not form around the full circumference of the bole in response to stressful conditions (Speer, 2010). Among datasets available through the International Tree-Ring Databank, an average 1 of 240 rings is absent, but this rate varies by species and latitude with maximum values in the Southwestern United States (2% absent, on average) or in trees of the genus *Pinus* (0.8% absent, on average) (St George *et al.*, 2013). This estimate is also conservative as St. George *et al*. (2013) searched for the often, but not universally applied, value of zero as an indicator of a missing ring. Rates can be much higher in the case of suppression or disease (Gutsell & Johnson, 2002; Black *et al.*, 2008a). False rings are generally caused by a stressful period during the growing season and can be distinguished through crossdating and careful inspection of wood anatomy (Speer, 2010). Rates vary greatly among species and site, and in extreme cases, false rings can occur in as many as a third (Copenheaver *et al.*, 2010b; Palakit *et al.*, 2012; Novak *et al.*, 2013; Novak *et al.*, 2014) to 80% of all increments (Marchand & Filion, 2012; Battipaglia *et al.*, 2014). Without crossdating, locally absent rings and false rings would contribute to the overall error rate, though additional error would almost certainly occur. For example, geoduck did not have true missing increments, but were consistently under-aged because increments were difficult to distinguish during periods of slow, suppressed growth (Black *et al.*, 2008b). Error rates in any species would increase in the case of poor sample preparation or reader inexperience.

Ultimately, the goal of this analysis was not to quantify error rates in studies performed without crossdating, but to demonstrate the effects of errors at what were likely conservative rates. The details of how those errors were inserted into measurement time series were likely unimportant to the results, though we attempted to follow rules that were as realistic as possible based on our experience. In practice, the probability of adding a “check” is generally greatest early in life and the probability of skipping a ring is greatest for narrow increments. Moreover, errors can occur while interpreting the partially formed increment at the known year of death, even in species with relatively clear increment patterns (Matta *et al.*, 2010). Also, increments are more often skipped than falsely added, resulting in consistent under-ageing (Black *et al.*, 2008b),

370 which was why 80% of errors were designated as missing rings in these simulation. Yet
371 regardless of the ratio of skipped to false rings, frame-shifts in the measurement time series will
372 attenuate the synchronous growth pattern and accumulate with increasing effect back through
373 time. Under the rules applied here, the high percentage of missed rings right-shifted the error
374 chronologies forward in time while a majority of false rings would have left-shifted error
375 chronologies backward in time. Either way, high-frequency followed by low-frequency
376 variability would be diminished or lost.
377
378 **Species-specific results**
379 Although the general effects were similar, error had somewhat different consequences in
380 each of the five species surveyed. For example, EPS in Douglas-fir did not steadily decline back
381 through time, but oscillated from the 1300s through the 1700s. This was almost certainly due to
382 synchronous low-frequency patterns that could have temporarily increased EPS, including sharp,
383 decadal-length suppressions consistent with the effects of insect outbreaks (Swetnam *et al.*,
384 1995; Flower *et al.*, 2014). Another example was the unusually pronounced difference between
385 the splitnose crossdated and error composite chronologies from approximately 1975 through the
386 end of the record. Synchrony among these individuals was strongly driven by unusually narrow
387 increments associated with potent El Niño events (Black *et al.*, 2011; Black *et al.*, 2014), two of
388 which (1983 and 1998) occurred in relatively quick succession late in the 20th century. These
389 extremes were prone to being heavily muted in the event of dating errors, markedly reducing
390 chronology accuracy and the magnitude of climate-growth relationships.
391
392 **Consequences of dating errors**
393 In the examples developed here, dating errors profoundly diminished relationships
394 between chronologies and environmental time series. This would complicate efforts to identify
395 key climatic drivers of growth, information critical to understanding species ecology and for
396 targeting variables for environmental reconstruction. Dating errors can lead to an
397 underestimation of the importance of climate as a determinant of interannual variability in tree
398 growth (Fig. 4) with implications for assessing the relative role and interaction of climate
399 change, management, and disturbances on current and projected forest productivity (Boisvenue
400 & Running, 2006). In this context, errors can propagate through the application of model-data

assimilation and allometric relations and thus increase uncertainty in the characterization of interacting climate and ecological influences (Becknell *et al.*, 2015). This is particularly relevant when estimating the potential of global forest ecosystems to function as carbon cycle source or sink under future climate change and thus when determining potential future forest-climate feedback mechanisms (Bonan, 2008).

Even if significant climate correlations are identified, as could happen in the event of low error rates, any estimates of variability prior to the start of the instrumental records could be highly inaccurate and could hamper accurate reconstruction of past climate. Accumulating error would give the illusion of a "smoother" climate signal as high-frequency variability is increasingly attenuated back through time. Moreover, extreme events would be lost, and variance may appear to rise over time as the reconstruction progresses from low-frequency variability in the early years to a combination of low- and high-frequency variability in the most recent years. Verifying reconstruction accuracy commonly involves a regression between the chronology and the instrumental record over the latter half of the interval shared by the two time series, and then testing that relationship using the independent, withheld data from the most recent half (or vice versa) (Fritts, 1976). This assessment of skill could be compromised by a steady decline in chronology quality that more strongly affects the early half of the data. Finally, if the rate of missed rings does not equal that of falsely added rings, reconstructions and the events they record will likely become offset in time. For example, major suppressions in Douglas-fir that occurred in the 1300s and 1400s were offset by as much as a decade at the 5% error rate (Fig. 2b). Additionally, age estimates would be biased; in an example from geoduck chronic under-ageing "smeared" what proved to be highly episodic recruitment events and underestimated the longevity of individuals at the site (Black *et al.*, 2008b). Thus, crossdating is important not just for retaining high-frequency phenomena, but also for estimating population age structure or reconstructing major disturbance events that leave profound, multi-year growth signatures. In all cases, such information is critical to estimating trends in central tendency and variance.

Importance of crossdating

Crossdating is a process of repeated hypothesis testing that resolves misidentifications in the growth-increment series by comparing synchronous patterns among individuals from a given

species and site. If a micro-ring, false ring, or locally absent ring is suspected, its presence can be tested by assessing whether the growth pattern has become offset by a year relative to that in the other samples, and then further confirmed by carefully re-examining the problematic increment. The challenge is identifying the synchronous pattern through individual-level variability and allowing the balance of evidence to guide the hypothesis testing process. Although crossdating generally involves increment width, other synchronous anatomical or chemical properties may be employed including false rings, frost rings, distinct earlywood or latewood signatures, luminance, density, isotopic, or geochemical composition (Hendy *et al.*, 2003; Roden, 2008; Anchukaitis & Evans, 2010; DeLong *et al.*, 2014). Importantly, crossdating is first and foremost a visual process that cannot yet be automated with computer programs. If the vast majority of samples have been visually crossdated correctly, then the contrast between the synchronous, population-wide signal and those few remaining samples that have errors will be maximized. In so doing, statistical analysis has the greatest power to identify these few dating mistakes. However, even if a sample is flagged by a quality-control program such as COFECHA, the final decision as to whether it is correctly dated can only be made upon visual re-inspection of the growth-increment structure (Grissino-Mayer, 2001).

When properly implemented, crossdating ensures that all increments are correctly placed in time, unlocking the power to fully integrate chronologies across species or sites, instrumental climate records, or other observational physical or biological time series (Black, 2009; Black *et al.*, 2011; Thompson *et al.*, 2012). Such analyses reveal how climate drives growth within and among species and its capacity to synchronize across broad spatial scales or across terrestrial, freshwater, and marine ecosystems (Rypel *et al.*, 2009; Black *et al.*, 2014). With crossdating, dead-collected or archival material can also be included to extend annually resolved environmental histories over multiple centuries or millennia (Pilcher *et al.*, 1984; Becker, 1993).

Crossdating limitations

Crossdating has important limitations. There must be a synchronous, annual signal in some attribute of the increment structure; increments that cannot be resolved, that do not vary from year to year, or that do not form on periodic (e.g. annual) timescales cannot be crossdated. Crossdating also requires adequate replication to ensure that the synchronous pattern is fully evident through individual-level “noise” and to ensure correct dating in the event that a large

463 percentage of samples has a growth irregularity (e.g. a false or locally absent ring) in a given
464 year (Fritts 1976, Wigley *et al*. 1984, Butler *et al*., 2009). Beyond its role in crossdating,
465 replication is also necessary to ensure that the final growth-increment chronology faithfully
466 captures the environmental signals that are the target of the reconstruction (Wigley *et al*., 1984;
467 Lough 2004).
468 In a sample set from a given species and site that displays interannual variability,
469 crossdating and assignment of the correct calendar year of formation can be reasonably assumed
470 if there is synchrony among individuals. This may be further corroborated by coherence across
471 multiple species or sites, and if the chronologies correlate to climate in a way that is consistent
472 with their ecology (Stahle, 1999). Radiometric techniques can provide independent validation of
473 increment periodicity and crossdating, with for example the time-specific pulse of ^{14}C fallout
474 ("bomb carbon") following nuclear testing in the late 1950s and early 1960s (Stahle, 1999;
475 Helser *et al.*, 2012; Scourse *et al.*, 2012). Yet even with networks of crossdated chronologies, it
476 has been hypothesized that errors could remain in the event of a widespread and therefore
477 unrecognized locally absent ring (Mann *et al.*, 2012). While this hypothesis has been refuted
478 (Anchukaitis *et al.*, 2012; Esper *et al*., 2013; St George *et al.*, 2013) and is very unlikely in a
479 large, well-replicated dataset, this possibility cannot be excluded by crossdating alone.
480 Advances in detecting global- or hemispheric-scale cosmogenic pulses in ^{14}C as occurred in
481 774/5 AD may provide a novel tool with which to independently validate annual accuracy in
482 millennial-length chronologies (Fowler, 2015).
483 As the purview of crossdating expands into animal growth increments, new challenges
484 arise. One of the most notable is that otoliths, shells, or other calcium carbonate structures do
485 not have cellular structure, which in trees can aid in identifying false rings or other anatomical
486 anomalies. Also, many of the animals used for crossdating are not sessile and could move across
487 regions of contrasting climate regimes over the course of a lifetime, which could complicate
488 attempts to crossdate (Ong *et al.*, 2015). Difference between sexes, especially with respect to
489 reproductive output or changing environmental requirements from juvenile to adult life stages
490 may also be important. Finally, the relatively short lifespan (20 < yr) of many animal species
491 limits the temporal pattern available to crossdate. Even if all samples are live collected, there is
492 little power to evaluate synchrony, let alone add individuals with unknown dates of death.

493 Finally, fish otoliths in particular can be highly "complacent" with minimal year-to-year
494 variability.
495 There is no substitution for visually matching patterns among samples and crossdating
496 must be applied whenever possible. However, multidecadal chronologies can still be constructed
497 from short-lived species using archives in which collection dates are known for all samples
498 (Black *et al.*, 2013; Morrongiello & Thresher, 2015). This strategy could be expanded
499 tremendously given century-long collections housed at various fishery agencies around the world
500 (Morrongiello *et al.*, 2012). Also, in the case of complacent sample sets, large numbers of
501 individuals can be measured to maximize common signal and generate highly climate-sensitive
502 chronologies (Rountrey *et al.*, 2014; Ong *et al.*, 2015). The point at which a sample set is too
503 complacent or short-lived to be considered truly crossdated is difficult to quantify. However, it
504 is clear that new criteria for estimating chronology quality and the impacts of error will be
505 necessary as these types of studies proliferate, especially considering the compelling results they
506 can produce. Minimal guidelines could include very high sample replication and accurate
507 characterization of uncertainties driven in part by the dating errors explored in this study.
508 Moreover, there may be cases where increment widths are relatively complacent, but chemical or
509 isotope signatures are synchronous and allow for greater confidence in ensuring correct calendar
510 dating (Roden, 2008).
511 In summary, dating errors impact chronology quality and underscore the importance of
512 crossdating to preserve signal strength and the frequency and severity of extreme events,
513 especially in high-frequency domains. The examples addressed here are all annual in
514 periodicity, though it is possible that crossdating could be applied at other timescales with for
515 example the daily increments formed in many bivalve and fish species (House & Farrow, 1968;
516 Morales-Nin, 2000). Crossdating is also relevant to proxy types other than growth increments
517 including ice cores, varves, and speleothems, though perhaps the greatest limitation is that
518 replicates can be relatively difficult and expensive to obtain (Comboul *et al.*, 2014). Where
519 multiple ice core or varved samples have been acquired, synchrony is apparent among supra-
520 annual features such as turbidites or volcanic ash horizons, though erosion, compression, and an
521 inability to match properties of each layer can complicate efforts to establish full annual
522 resolution (Weinheimer & Biondi, 2003; Vinther *et al.*, 2006). Speleothem records have been
523 correlated to one another within and among caves or with other proxies (Trouet *et al.*, 2009),

524 though efforts to fully crossdate them to annual resolution have rarely been attempted (Baker *et*
525 *al.*, 2015), and they mostly prove difficult to verify against annually resolved climate records
526 (Betancourt *et al.*, 2002; Asmerom & Polyak, 2004). In comparison to growth-increment data
527 these proxies often provide much greater temporal depth and occur in environments where
528 growth increments are unavailable, with for example the polar ice caps. Crossdating may prove
529 useful under the correct circumstances and may be facilitated with greater sample depth.
530 Ultimately, however, crossdating is clearly practical across a wide and rapidly broadening range
531 of data types, and the diversity of these annually-resolved records will not only facilitate multi-
532 proxy environmental reconstructions, but also attempts to better understand ecosystem-level
533 responses to climate forcing.
534

535 ## Acknowledgements

536 BAB was supported by NSF grant OCE 1434732 as well as the HJ Andrews Experimental Forest
537 research program, funded by the National Science Foundation's Long-Term Ecological Research
538 Program (DEB 1440409), US Forest Service Pacific Northwest Research Station, and Oregon
539 State University. ADW was supported by NSF Grant OCE-1003438. BMG was supported by an
540 ARC Future Fellowship (FT100100767). We thank A. Tepley, S. Shafer, and R. Kormanyos for
541 assistance in developing the Browder Creek Douglas-fir chronology.
542

543 ## References

544 Anchukaitis KJ, Breitenmoser P, Briffa KR *et al.* (2012) Tree rings and volcanic cooling. *Nature*
545 *Geoscience*, **5**, 836-837.
546 Anchukaitis KJ, Evans MN (2010) Tropical cloud forest climate variability and the demise of the
547 Monteverde golden toad. *Proceedings of the National Academy of Sciences of the United*
548 *States of America*, **107**, 5036-5040.
549 Asmerom Y, Polyak VJ (2004) A test of annual resolution in stalagmites using tree rings.
550 *Quaternary Research*, **61**, 119-121.
551 Austin WEN, Bard E, Hunt JB, Kroon D, Peacock JD (1995) The C-14 age of the Icelandic
552 Vedde Ash - Implications for Younger-Dryas marine reservoir age corrections.
553 *Radiocarbon*, **37**, 53-62.

554 Baker A, Hellstrom JC, Kelly BFJ, Mariethoz G, Trouet V (2015) A composite annual-resolution
555 stalagmite record of North Atlantic climate over the last three millennia. *Scientific*
556 *Reports,* **5**, doi:10.1038/srep10307.
557 Baker A, Smart PL, Edwards RL, Richards DA (1993) Annual growth banding in a cave
558 stalagmite. *Nature,* **364**, 518-520.
559 Battipaglia G, Demicco V, Brand WA, Saurer M, Aronne G, Linke P, Cherubini P (2014)
560 Drought impact on water use efficiency and intra-annual density fluctuations in *Erica*
561 *arborea* on Elba (Italy). *Plant, Cell, & Environment,* **37**, 382-391.
562 Baumgartner TR, Michaelsen J, Thompson LG, Shen GT, Soutar A, Casey RE (1989) The
563 recording of interannual climatic change by high-resolution natural systems: Tree-rings,
564 coral bands, glacial ice layers, and marine varves. In: *Aspects of Climatic Variability in*
565 *the Pacific and the Western Americas.* (ed Peterson DH) pp 1-14. American Geophysical
566 Union.
567 Becker B (1993) An 11,000-year German oak and pine dendrochronology for radiocarbon
568 calibration. *Radiocarbon,* **35**, 201-213.
569 Becknell JM, Desai AR, Dietze MC *et al.* (2015) Assessing interactions among changing
570 climate, management, and disturbance in forests: A macrosystems approach. *Bioscience,*
571 **65**, 263-274.
572 Betancourt JL, Grissino-Mayer HD, Salzer MW, Swetnam TW (2002) A test of "annual
573 resolution" in stalagmites using tree rings. *Quaternary Research,* **58**, 197-199.
574 Black BA (2009) Climate driven synchrony across tree, bivalve, and rockfish growth-increment
575 chronologies of the northeast Pacific. *Marine Ecology Progress Series,* **378**, 37-46.
576 Black BA, Boehlert GW, Yoklavich MM (2005) Using tree-ring crossdating techniques to
577 validate annual growth increments in long-lived fishes. *Canadian Journal of Fisheries*
578 *and Aquatic Sciences,* **62**, 2277-2284.
579 Black BA, Colbert JJ, Pederson N (2008a) Relationships between radial growth rates and
580 lifespan within North American tree species. *Ecoscience,* **15**, 349-357.
581 Black BA, Copenheaver CA, Frank DC, Stuckey MJ, Kormanyos RE (2009) Multi-proxy
582 reconstructions of northeastern Pacific sea surface temperature data from trees and
583 Pacific geoduck. *Palaeogeography Palaeoclimatology Palaeoecology,* **278**, 40-47.

584 Black BA, Gillespie D, Maclellan SE, Hand CM (2008b) Establishing highly accurate
585 production-age data using the tree-ring technique of crossdating: a case study for Pacific
586 geoduck (*Panopea abrupta*). *Canadian Journal of Fisheries and Aquatic Sciences,* **65**,
587 2572-2578.
588 Black BA, Matta ME, Helser TE, Wilderbuer TK (2013) Otolith biochronologies as multidecadal
589 indicators of body size anomalies in yellowfin sole (Limanda aspera). *Fisheries*
590 *Oceanography,* **22**, 523-532.
591 Black BA, Schroeder ID, Sydeman WJ, Bograd SJ, Wells BK, Schwing FB (2011) Winter and
592 summer upwelling modes and their biological importance in the California Current
593 Ecosystem. *Global Change Biology,* **17**, 2536-2545.
594 Black BA, Sydeman WJ, Frank DC *et al.* (2014) Six centuries of variability and extremes in a
595 coupled marine-terrestrial ecosystem. *Science,* **345**, 1498-1502.
596 Boisvenue C, Running SW (2006) Impacts of climate change on natural forest productivity -
597 evidence since the middle of the 20th century. *Global Change Biology,* **12**, 862-882.
598 Bonan GB (2008) Forests and climate change: Forcings, feedbacks, and the climate benefits of
599 forests. *Science*, **320**, 1444-1449.
600 Butler PG, Richardson CA, Scourse JD *et al.* (2009) Accurate increment identification and the
601 spatial extent of the common signal in five Arctica islandica chronologies from the
602 Fladen Ground, northern North Sea. *Paleoceanography*, **24**, doi:10.1029/2008PA001715.
603 Butler PG, Wanamaker AD, Scourse JD, Richardson CA, Reynolds DJ (2013) Variability of
604 marine climate on the North Icelandic Shelf in a 1357-year proxy archive based on
605 growth increments in the bivalve *Arctica islandica*. *Palaeogeography Palaeoclimatology*
606 *Palaeoecology*, **373**, 141-151.
607 Ciais P, Reichstein M, Viovy N *et al.* (2005) Europe-wide reduction in primary productivity
608 caused by the heat and drought in 2003. *Nature*, **437**, 529-533.
609 Cobb KM, Charles CD, Cheng H, Edwards RL (2003) El Nino/Southern Oscillation and tropical
610 Pacific climate during the last millennium. *Nature,* **424**, 271-276.
611 Comboul M, Emile-Geay J, Evans MN, Mirnateghi N, Cobb KM, Thompson DM (2014) A
612 probabilistic model of chronological errors in layer-counted climate proxies: applications
613 to annually banded coral archives. *Climate of the Past,* **10**, 825-841.

614 Cook ER, Holmes RL (1986) User manual for program ARSTAN. In: *Tree-Ring Chronologies*
615 *of Western North America: California, Eastern Oregon and Northern Great Basin with*
616 *Procedures Used in the Chronology Development Work Including Users Manuals for*
617 *Computer Programs COFECHA and ARSTAN*. (eds Holmes RL, Adams RK, Fritts HC)
618 pp 50-65. Tucson, AZ, Laboratory of Tree-Ring Research, University of Arizona.
619 Cook ER, Krusic PJ (2005) *ARSTAN v. 41d: A tree-ring standardization program based on*
620 *detrending and autoregressive time series modeling, with interactive graphics*, Palisades,
621 New York, USA, Tree-Ring Laboratory, Lamont-Doherty Earth Observatory of
622 Columbia University.
623 Copenheaver CA, Gartner H, Schafer I, Vaccari FP, Cherubini P (2010a) Drought-triggered false
624 ring formation in a Mediterranean shrub. *Botany-Botanique*, **88**, 545-555.
625 Copenheaver CA, Gärtner H, Schäfer I, Vaccari FP, Cherubini P (2010b) Drought triggered false
626 ring formation in a Mediterranean shrub. *Botany-Botanique*, **88**, 545-555.
627 Delong KL, Flannery JA, Poore RZ, Quinn TM, Maupin CR, Lin K, Shen CC (2014) A
628 reconstruction of sea surface temperature variability in the southeastern Gulf of Mexico
629 from 1734 to 2008 CE using cross-dated Sr/Ca records from the coral Siderastrea siderea.
630 *Paleoceanography*, **29**, 403-422.
631 Douglass AE (1941) Crossdating in dendrochronology. *Journal of Forestry*, **39**, 825-831.
632 Edmondson JR (2010) The Meteorological Significance of False Rings in Eastern Redcedar
633 (Juniperus Virginiana L.) from the Southern Great Plains, USA. *Tree-Ring Research*, **66**,
634 19-33.
635 Esper J, Büntgen U, Luterbacher J, Krusic PJ (2013) Testing the hypothesis of post-volcanic
636 missing rings in temperature sensitive dendrochronological data. *Dendrochronologia*, **31**,
637 216-222.
638 Ferguson CW, Lawn B, Michael HN (1985) Prospects for the extension of the bristlecone pine
639 chronology - radiocarbon analysis of H-84-1. *Meteoritics*, **20**, 415-421.
640 Flower A, Gavin DG, Heyerdahl EK, Parsons RA, Cohn GM (2014) Drought-triggered western
641 spruce budworm outbreaks in the interior Pacific Northwest: A multi-century
642 dendrochronological record. *Forest Ecology and Management*, **324**, 16-27.
643 Foster DR, Knight DH, Franklin JF (1998) Landscape patterns and legacies resulting from large,
644 infrequent forest disturbances. *Ecosystems*, **1**, 497-510.

Fowler AM (2015) Are cosmogenic events about to revolutionise the crossdating of multi-millennial tree-ring chronologies? *Dendrochronologiea,* **35**, 1-3.

Friedrich M, Remmelel S, Kromer B *et al.* (2004) The 12,460-year Hohenheim oak and pine tree-ring chronology from central Europe - A unique annual record for radiocarbon calibration and paleoenvironment reconstructions. *Radiocarbon,* **46**, 1111-1122.

Fritts HC (1976) *Tree Rings and Climate,* New York, Academic Press.

Fritts HC, Swetnam TW (1989) Dendroecology - a Tool for Evaluating Variations in Past and Present Forest Environments. *Advances in Ecological Research,* **19**, 111-188.

Glock WS (1937) *Principles and Methods of Tree-Ring Analysis,* Washington, D. C., Carnegie Institution of Washington.

Griffin SM (2012) Applying dendrochronology visual crossdating techniques to the marine bivalve *Arctica islandica* and assessing the utility of master growth chronologies as proxies for temperature and secondary productivity in the Gulf of Maine. Unpublished MS Iowa State Univresity, Ames, IA, 237 pp.

Grinsted A, Moore JC, Jevrejeva S (2004) Application of the cross wavelet transform and wavelet coherence to geophysical time series. *Nonlinear Processes in Geophysics,* **11**, 561-566.

Grissino-Mayer HD (2001) Evaluating crossdating accuracy: a manual and tutorial for the computer program COFECHA. *Tree-Ring Research,* **57**, 205-221.

Grissino-Mayer HD, Fritts HC (1997) The International Tree-Ring Data Bank: An enhanced global database serving the global scientific community. *Holocene,* **7**, 235-238.

Gutsell SL, Johnson EA (2002) Accurately ageing trees and examining their height-growth rates: implications for interpreting forest dynamics. *Journal of Ecology,* **90**, 153-166.

Helser TE, Lai HL, Black BA (2012) Bayesian hierarchical modeling of Pacific geoduck growth increment data and climate indices. *Ecological Modelling,* **247**, 210-220.

Hendy EJ, Gagan MK, Lough JM (2003) Chronological control of coral records using luminescent lines and evidence for non-stationary ENSO teleconnections in northeast Australia. *Holocene,* **13**, 187-199.

Holmes RL (1983) Computer-assisted quality control in tree-ring dating and measurement. *Tree-Ring Bulletin,* **43**, 69-78.

675 House MR, Farrow GE (1968) Daily growth banding in shell of cockle *Cardium edule*. *Nature,*
676 **219**, 1384-1386.
677 Jackson ST, Betancourt JL, Booth RK, Gray ST (2009) Ecology and the ratchet of events:
678 Climate variability, niche dimensions, and species distributions. *Proceedings of the*
679 *National Academy of Sciences of the United States of America,* **106**, 19685-19692.
680 LDEO (2015) Lamont-Doherty Earth Observatory. ARSTAN download.
681 http://www.ldeo.columbia.edu/tree-ring-laboratory/resources/software.
682 Lowe J, Walker M (2015) Measuring Quaternary time: A 50-year perspective. *Journal of*
683 *Quaternary Science*, **30**, 104-113.
684 Lough JM (2004) A strategy to improve the contribution of coral data to high-resolution
685 paleoclimatology. *Palaeogeography Palaeoclimatology Palaeoecology*, **204**, 115-143.
686 Mann ME, Fuentes JD, Rutherford S (2012) Underestimation of volcanic cooling in tree-ring-
687 based reconstructions of hemispheric temperatures. *Nature Geoscience,* **5**, 202-205.
688 Marchand N, Filion L (2012) False rings in the white pine (*Pinus strobus)* of the Outaouais Hills,
689 Quebec (Canada), as indicators of water stress. *Canadian Journal of Forest Research,* **42**,
690 12-22.
691 Matta ME, Black BA, Wilderbuer TK (2010) Climate-driven synchrony in otolith growth-
692 increment chronologies for three Bering Sea flatfish species. *Marine Ecology-Progress*
693 *Series,* **413**, 137-145.
694 Mette MJ, Wanamaker AD, Carroll ML, Ambrose WG, Retelle MJ (2016) Linking large-scale
695 climate variability with *Arctica islandica* shell growth and geochemistry in northern
696 Norway, *Limnology and Oceanography*, doi:10.1002/lno.10252.
697 Morales-Nin B (2000) Review of the growth regulation processes of otolith daily increment
698 formation. *Fisheries Research*, **46**, 53-67.
699 Morrongiello JR, Thresher RE (2015) A statistical framework to explore ontogenetic growth
700 variation among individuals and populations: a marine fish example. *Ecological*
701 *Monographs,* **85**, 93-115.
702 Morrongiello JR, Thresher RE, Smith DC (2012) Aquatic biochronologies and climate change.
703 *Nature Climate Change,* **2**, 849-857.

704 Novak K, Deluís M, Raventós J, Čufar K (2014) Climatic signals in tree-ring widths and wood
705 structure of *Pinus halepensis* in contrasted environmental conditions. *Trees Structure and*
706 *Function*, **27**, 927-936.
707 Novak K, Saz-Sanchez MA, Cufar K, Raventos J, De Luis M (2013) Age, climate and intra-
708 annual density fluctuations in *Pinus halepensis* in Spain. *IAWA Journal*, **34**, 459-474.
709 Ong JJL, Rountrey AN, Meeuwig JJ, Newman SJ, Zinke J, Meekan MG (2015) Contrasting
710 environmental drivers of adult and juvenile growth in a marine fish: implications for the
711 effects of climate change. *Scientific Reports*, **5**, doi: 10.1038/srep10859.
712 Palakit K, Siripattanadilok S, Duangsathaporn K (2012) False ring occurrences and their
713 identification in teak (*Tectonia grandis*) in north-eastern Thailand. *Journal of Tropical*
714 *Forest Science*, **24**, 387-398.
715 Pilcher JR, Baillie MGL, Schmidt B, Becker B (1984) A 7,272-year tree-ring chronology for
716 western Europe. *Nature*, **312**, 150-152.
717 Reichstein M, Bahn M, Ciais P *et al.* (2013) Climate extremes and the carbon cycle. *Nature*, **500**,
718 287-295.
719 Roden J (2008) Cross-dating of tree ring delta O-18 and delta C-13 time series. *Chemical*
720 *Geology*, **252**, 72-79.
721 Rountrey AN, Coulson PG, Meeuwig JJ, Meekan M (2014) Water temperature and fish growth:
722 otoliths predict growth patterns of a marine fish in a changing climate. *Global Change*
723 *Biology*, **20**, 2450-2458.
724 Rypel AL, Haag WR, Findlay RH (2009) Pervasive hydrologic effects on freshwater mussels
725 and riparian trees in southeastern floodplain ecosystems. *Wetlands*, **29**, 497-504.
726 Schulman E (1939) Classification of false annual rings in West Texas pines. *Tree-Ring Bulletin*,
727 **6**, 11-13.
728 Scott EM, Cook GT, Naysmith P (2007) Error and uncertainty in radiocarbon measurements.
729 *Radiocarbon*, **49**, 427-440.
730 Scourse J, Richardson C, Forsythe G et al. (2006) First cross-matched floating chronology from
731 the marine fossil record: data from growth lines of the long-lived bivalve mollusc *Arctica*
732 *islandica*. *Holocene*, **16**, 967-974.

733 Scourse JD, Wanamaker AD, Weidman C *et al.* (2012) *The marine radiocarbon bomb Pulse*
734 *across the temperate North Atlantic: a compilation of delta C-14 time histories from*
735 *Arctica islandica growth increments*. *Radiocarbon*, **54**, 165-186.
736 Speer JH (2010) *Fundamentals of Tree-Ring Research,* Tucson, University of Arizona Press.
737 St George S (2014) An overview of tree-ring width records across the Northern Hemisphere.
738 *Quaternary Science Reviews*, **95**, 132-150.
739 St George S, Ault TR, Torbenson MCA (2013) The rarity of absent growth rings in Northern
740 Hemisphere forests outside the American Southwest. *Geophysical Research Letters,* **40**,
741 3727-3731.
742 Stahle DW (1999) Useful strategies for the development of tropical tree-ring chronologies. *IAWA*
743 *Journal,* **20**, 249-253.
744 Stahle DW, Griffin RD, Meko DM *et al.* (2013) The ancient blue oak woodlands of California:
745 longevity and hydro-climatic history. *Earth Interactions,* **17**, 1-12.
746 Stokes MA, Smiley TL (1996) *An Introduction to Tree-Ring Dating,* Tucson, Arizona, The
747 University of Arizona Press.
748 Strom A, Francis RC, Mantua NJ, Miles EL, Peterson DL (2004) North Pacific climate recorded
749 in growth rings of geoduck clams: A new tool for paleoenvironmental reconstruction.
750 *Geophysical Research Letters,* **31**, doi:10.1029/2004GLO19440.
751 Swetnam TW, Wickman BE, Paul HG, Baisan CH (1995) Historical patterns of western spruce
752 budworm and Douglas-fir tussock moth outbreaks. pp 35, Washington, DC, USDA
753 Forest Service.
754 Thompson SA, Sydeman WJ, Santora JA *et al.* (2012) Linking predators to seasonality of
755 upwelling: Using food web indicators and path analysis to infer trophic connections.
756 *Progress in Oceanography,* **101**, 106-120.
757 Trouet V, Esper J, Graham NE, Baker A, Scourse JD, Frank DC (2009) Persistent positive North
758 Atlantic Oscillation mode dominated the Medieval Climate Anomaly. *Science*, **324**, 78-
759 80.
760 Trouet V, Van Oldenborgh GJ (2013) KNMI Climate Explorer: A web-based research tool for
761 high-resolution paleoclimatology. *Tree-Ring Research,* **69**, 3-13.
762 Vinther BM, Clausen HB, Johnsen SJ *et al.* (2006) A synchronized dating of three Greenland ice
763 cores throughout the Holocene. *Journal of Geophysical Research-Atmospheres,* **111**.

764 Weinheimer A, Biondi F (2003) Paleoclimatology: Varves. In: *Encyclopedia of Atmospheric*
765 *Sciences.* (eds Holton JR, Pye JA, Curry JA) pp 1680–1684. London, Academic Press.
766 Wigley TML, Briffa KR, Jones PD (1984) On the average value of correlated time-series, with
767 applications in dendroclimatology and hydrometeorology. *Journal of Climate and*
768 *Applied Meteorology*, **23**, 201-213.
769

770 Supporting Information captions

771 Figure S1. Cross-wavelet analysis of the crossdated chronology and the mean of 100 simulation
772 runs at a 1% error rate for blue oak, Douglas-fir, *Arctica*, geoduck, and splitnose rockfish.
773
774 Figure S2. Sample depth (number of individuals) and the expressed population signal (EPS) for
775 the correctly dated chronology, and the mean of 100 simulation runs at 1% and 5% error rates for
776 blue oak, Douglas-fir, *Arctica*, geoduck, and splitnose rockfish.
777
778 Figure S3. Correlation coefficient between each of three "floating" samples of unknown death
779 date and master chronologies that have no dating error, 1% error rates, and 5% error rates.
780

781
782 *Table 1. Growth-increment data attributes.*

Species	N individuals[1]	N meas. time ser.[2]	span[3]	mean length[4]	SIC[5]
Blue oak	62	74	1787-2003	136	0.84
Douglas-fir	30	30	1266-2006	664	0.57
Arctica	14	14	1926-2009	82	0.73
Geoduck	34	17	1924-2002	52	0.74
Splitnose rockfish	70	70	1931-2007	37	0.58

783
784 [1] Number of individuals
785 [2] Number of measurement time series
786 [3] Span of the final chronology with a minimum of five individuals contributing

[4] Mean length (years) of the measurement time series

[5] Mean series intercorrelation as calculated by COFECHA

Figure Captions

Figure 1. Crossdated and error chronologies for blue oak. (a) The mean chronology and crossdated measurement time series for blue oak. (b) The same blue oak measurement time series with a 5% error rate in dating. Black line is the resulting 5% error chronology. (c) The 5% error simulation was run 100 times, and each of the 100 mean chronologies is shown, as is their composite mean (black line) and the correctly dated chronology from Panel (a) (blue line).

Figure 2. The correctly dated chronology and the composite chronology as averaged across 100 simulation runs at 1% and 5% error rates. The probability density functions of growth-increment index (GI) values are also shown for each of the three chronologies. Lower panel is percentage of correctly dated measurement time series, as averaged across 100 simulation runs at 1% and 5% error rates. (a) blue oak, (b) Douglas-fir, (c) *Arctica*, (d) geoduck, and (e) splitnose rockfish. Note that the x and y axes vary for each chronology.

Figure 3. Cross-wavelet analysis of the crossdated chronology and the mean of 100 simulation runs at a 5% error rate for (a) blue oak, (b) Douglas-fir, (c) *Arctica*, (d) geoduck, and (e) splitnose rockfish. Color represents signal power and the arrows indicate the direction of the correlation (right pointing = positively phased; left pointing = negatively phased). Contours show significant relationships at the $p < 0.05$ level in comparison to a red noise spectrum. Shaded areas are a cone of influence in which edge effects are present.

Figure 4. Climate-chronology relationships. a, d, g) Correlation coefficient between climate and the correctly dated chronology (no error); also mean and 99% confidence interval for the correlation between climate and each of the 100 simulation runs at 1% error rates (1%), and 5% error rates (5%). a) Correlations between blue oak and winter (prior Dec – Feb) precipitation in NOAA NCDC CA divisions 5 and 7. Correlations between gridded winter precipitation and b) the correctly dated blue oak chronology and c) the blue oak composite 5% error chronology. d)

818 Correlations between the geoduck chronology and British Columbia sea surface temperatures
819 (SST). Correlations between gridded mean annual SST and e) the correctly dated geoduck
820 chronology and, f) the geoduck composite 5% error chronology. g) Correlations between
821 splitnose rockfish and winter upwelling averaged across 36°N and 39°N. Correlations between
822 gridded winter SST (an index of upwelling) and the h) correctly dated splitnose chronology and,
823 i) the splitnose composite 5% error chronology.
824
825 Figure 5. Effects of error on detection of extremes defined as values > 2 standard deviations from
826 the mean. (a) Blue oak crossdated chronology normalized to a mean of zero and standard
827 deviation of one. Five years exceed 2 standard deviations (extend into gray shaded area): 1801,
828 1826, 1838, 1868, and 1937. (b) Percentage of 100 simulation runs at 1% dating error rate that
829 correctly identify an extreme event; also the percentage of runs that falsely detect an extreme
830 event (false positives). (c) Results at the 5% dating error rate.

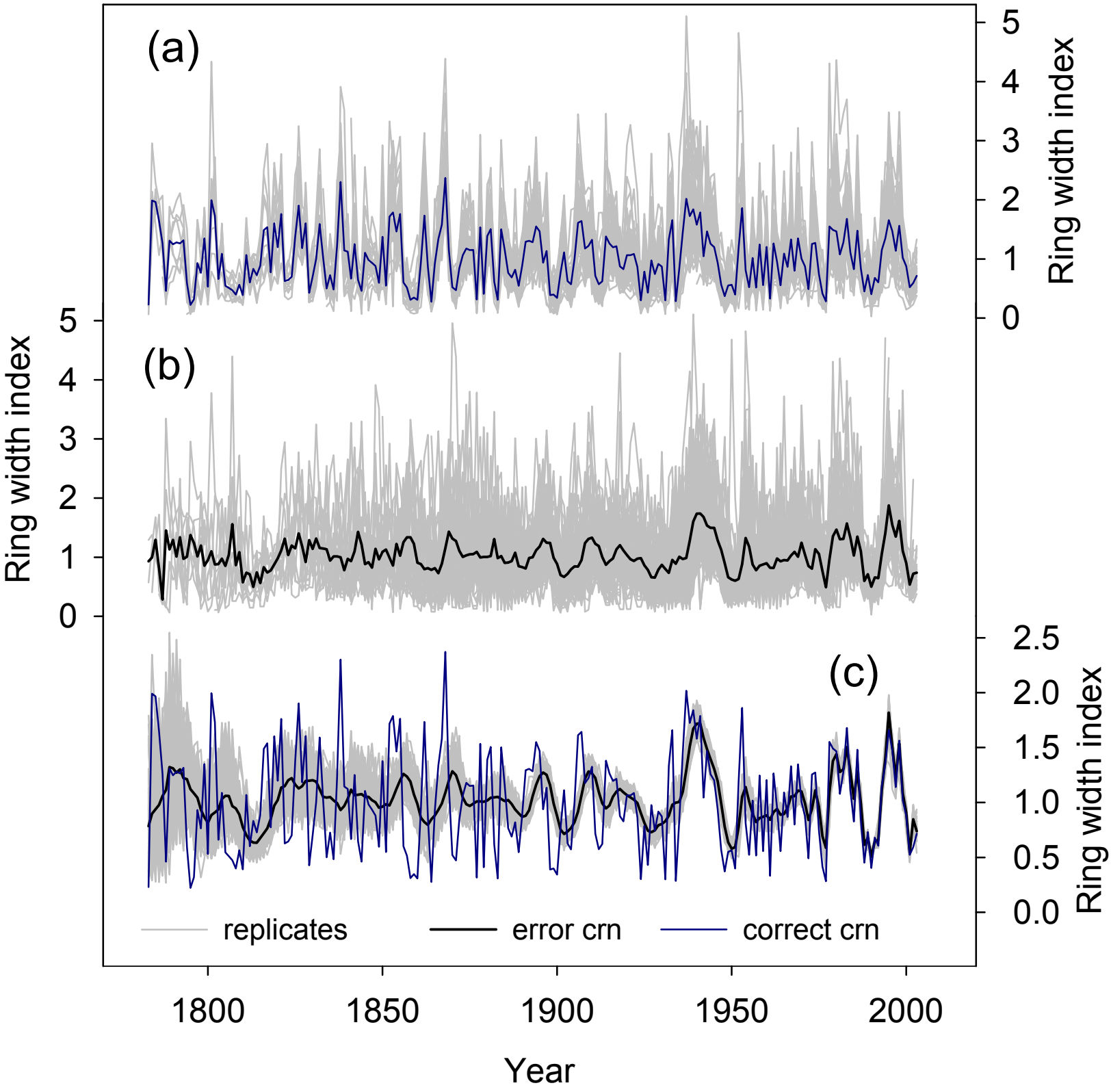

gcb_13256_f1.eps